TWELFTH EUROPEAN ROTORCRAFT FORUM

Paper No. 80.

DESCRIPTION OF, AND PRELIMINARY RESULTS FROM, A NEW BLADE-VORTEX INTERACTION TEST FACILITY

A. Kokkalis
R.A.McD. Galbraith

Department of Aeronautics and Fluid Mechanics,
UNIVERSITY OF GLASGOW,
GLASGOW, U.K.

September 22-25, 1986.

Garmisch-Partenkirchen,
Federal Republic of Germany.

Deutsche Gesellschaft fur Luft-und Raumfahrt e.V. (DGLR)
Godesberger Allee 70, D-5300 Bonn 2, F.R.G.

DESCRIPTION OF, AND PRELIMINARY RESULTS FROM, A NEW BLADE-VORTEX INTERACTION TEST FACILITY

A. Kokkalis and R.A.McD. Galbraith

SUMMARY

The paper describes the salient design features of a facility for the investigation of parallel blade-vortex interaction as may be experienced by helicopter rotor blades. Preliminary results from the test facility are presented and discussed.

NOMENCLATURE

a	Local speed of sound
c	Blade chord
$C_{m1/4}$	Pitching moment coefficient at 1/4-chord
C_n	Normal force coefficient
C_p	Pressure coefficient ($p/0.5\rho V_r^2$)
h	Radial distance from the center of the vortex
M_L	Local Mach number (V_r/a)
Nv	Number of values recorded
p	Surface pressure
r	Radius of a spanwise station from center of blade rotation
R	Blade tip radius
Re	Reynolds number ($V_r c/\nu$)
U	Free stream velocity
V_r	Rotational velocity at spanwise station ($2\pi\omega r$)
Γ	Vortex strength
δ	Angle-of-attack of vortex generator
Ψ	Azimuthal position of blade
ω	Angular speed of blade

INTRODUCTION

Any finite lifting surface produces a trailing system of vortices as a consequence of the wing loading and Helmotz continuation (second) law. Such a system usually takes the form of a variable strength vortex sheet shed from the trailing edge of the lifting surface and which then rolls-up into discrete vortices. For the particular case of a helicopter rotor blade, such vortices trail from the rotor hub and tip. For certain flight conditions, the strong vortex originating from the tip of one blade interacts with the following blade (Fig. 1). Such interactions induce significant changes in the blade circulation and hence changes in blade loading. These induced airloads have been identified as being major contributors to helicopter fuselage vibrations and radiated aerodynamic noise. The prediction of vortex induced airloads is therefore desirable.

To date, a number of computational methods to assess such interactions have been devised. These are generally based on finite-difference schemes that emulate the interaction of an ideal two-dimensional vortex with a finite aerofoil (Refs. 1,2). These techniques, however, have met with limited success, not least because of of the dearth of corraborative experimental data. In particular, the experimental investigation of a

Each airfoil section had a 150 mm chord and a semispan of 750 mm. The vortex strength, Γ, was varied by setting the airfoils at equal but opposite angles of attack, δ. The relative vertical position of the vortex to the rotor blade, h/c (+ve above), was adjusted by relocating the generator juncture via a re-alignment of small blade element (see Fig 3).

The vortex was located by means of oil-smoke flow visualisation and subsequent measurements of the flow field were by means of a triple C.T.A. probe.

2.2 Rotor Assembly

A diagram of the rotor assembly and its supports are shown in Fig. 2 . This arrangement was chosen because of its simple symmetric design, construction and minimal wind tunnel blockage effects. The single straight blade had a NACA 0015 profile, a chord of 150 mm and an aspect ratio of 5. The blade components were C.N.C. machined from Duralumin plate (as shown in Fig. 4) and resulted in a stiff model. The first flap and torsional frequencies were calculated (Ref. 7) to be 27 Hz and 163 Hz respectively, and the maximum tip deflection was 3.2 mm for the worst predicted loading case. Blade motion effects upon the measured data were therefore kept to a minimum. The blade incidence was set at zero degrees which further simplified the interaction considered, since the loadings would be primarily caused by the BVI. Furthermore, any vortex distortion due to the blade incidence/loading would be minimal.

The outer 50% of the blade's span was so designed as to incoporate an intrumentation pod (Fig. 5) containing 24 pressure transducers. This pod could be positioned so that the transducers were located at any of the spanwise positions r/R of 0.55, 0.65, 0.75, 0.85 and 0.95. To date, measurements have been made with the transducers located at r/R = 0.75 and r/R = 0.95. The chordwise distribution of the individual pressure transducers around the airfoil section is given in Table 1 . A further 2 pressure transducers were located at r/R=0.75 and 0.85 and at a distance of 0.03C from the leading edge on the upper surface. These were to assist in the assessment of the interaction's parallelism.

The blade was fixed at the rotor hub and statically balanced by means of counterweights. Once balanced, the rotor assembly was secured on 100 mm O.D. supports of high tensile steel tubing positioned at the center-line of the tunnel's test section. The blade rotation was obtained via a 3:1 ratio straight bevel gear coupled to a 1.5 Kw thyristor controlled D.C. electric motor.

2.3. Electronic Instrumentation

A block diagram of the various electronic instruments used and their interconnections is shown in Fig. 6 . The output from the Incremental Optical Encoder (Ferranti type 24QB) was passed to an electronic decoder/counter where it was conditioned to generate two signals. The first was used for logging the azimuthal angle of the blade. The second was linked to the external trigger input of the A-to-D convertor and provided the start pulse for the data acquisition sequence.

were taken. During the transfer to store the data were converted from the recorders format to Real numbers and the task was monitored to identify any associated data problems. At the end of each session, the data were put on magnetic tape for transfer to a VAX 11/750 computer.

Post run software consisted of data reduction, data analysis and data presentation routines. The data reduction routine reduced the raw data to non-dimensional pressure coefficients whilst the data analysis routine integrated the pressure coefficients to obtain Normal force and 1/4-chord Pitching moment coefficients. During this process, averaging of each of these quantities over the recorded number of cycles was carried out. After reduction of the data to the basic form of C_p, C_n, and $C_{m1/4}$ graphical routines performed all the necessary illustrations, etc. (e.g. Fig. 10.) .

RESULTS AND DISCUSSION

Of the extensive amount of data collected for various values of Γ and h/c, only a few representative results are presented herein. These are for one value of Γ (i.e. corresponding to δ=7.5°) and for r/R=0.95 with the vortex located at h/c=+0.20 .

As part of the preliminary investigation to assess the vortex structure and trajectory, oil-smoke flow visualization was used and the resulting streak lines recorded on photographic film. For the case considered here (δ=7.5°), a typical photographic record of the vortex is given in Fig. 8. It may be observed that the vortex rols-up close to the wing and has a well defined symmetrical structure. Furthermore, there was very little vortex meander and the trajectory was well defined. It had originally been intended to include measurements of the vortex strength but, due to limitations in computer processing time available, the acquired data awaits reduction.

Since the vortex interaction is of short duration (0.9 msecs), it is prudent to assess the data repeatability to be confident that the BVI will not be lost in the averaging process employed. Typical unsteady pressure traces from x/c=0.050 of upper surface and four h/c positions, are presented in Fig. 9, where it may be observed that the signals show excellent correlation both in magnitude and spatial repetition; the BVI event is evident.

The azimuthal variation of the upper surface C_p, normal force and 1/4-chord pitching moment coefficients for h/c=+0.20 and r/R=0.95, is presented in Fig. 10(a-c). It may be observed (Fig. 10a) that the most important effect of the BVI at Ψ=180°, is the sharp C_p perturbation in the leading edge region. This shows that the pressure increases as the vortex approaches the leading edge and then decreases as the vortex moves away. Similar trends are also evident in the azimuthal variation of C_n (Fig. 10b), but no such trend was observed in $C_{m1/4}$ (Fig. 10c). The $C_{m1/4}$ time history may be expected since (also noted in Ref. 5) the most prominent pressure variations due to BVI occur in the first 20% of blade chord and so, even significant C_p variations will have little contribution to 1/4-chord pitching moments when compared to minor C_p variations at the trailing edge. It is suggested that the evidently small and apparently random C_p perturbations in the region of trailing edge (Fig. 10a), are

5. F.X. Caradonna, G.H. Laub, C. Tung — An Experimental Investigation of the Parallel Blade-Vortex Interaction. 10th European Rotorcraft Forum, The Hague, The Netherlands, Aug. 1984.

6. G. Neuwerth, R. Muller — Pressure Fluctuations on Rotor Blades generated by Blade-Vortex Interaction. 10th European Rotorcraft Forum, The Hague, The Netherlands, Aug. 1984.

7. P. Juggins — Private Communication Westland Helicopters, Yeovil, U.K.

8. M. Surendraiah — An experimental Study of Rotor Blade-Vortex Interaction. NASA CR-1573, 1970.

x/c at -			
r/R = 0.75		r/R = 0.95	
Upper Surface	Lower Surface	Upper Surface	Lower Surface
0.000	0.007	0.000	0.007
0.015	0.030	0.015	0.030
0.030	0.060	0.050	0.060
0.050	0.100	0.075	0.150
0.075	0.150	0.100	0.350
0.100	0.200	0.125	0.550
0.125	0.350	0.200	0.760
0.150	0.550	0.350	0.920
0.200	0.760	0.550	
0.350	0.920	0.760	
0.550		0.860	
0.760		0.950	
0.860			
0.950			

TABLE 1: CHORDWISE PRESSURE-TRANSDURE LOCATIONS

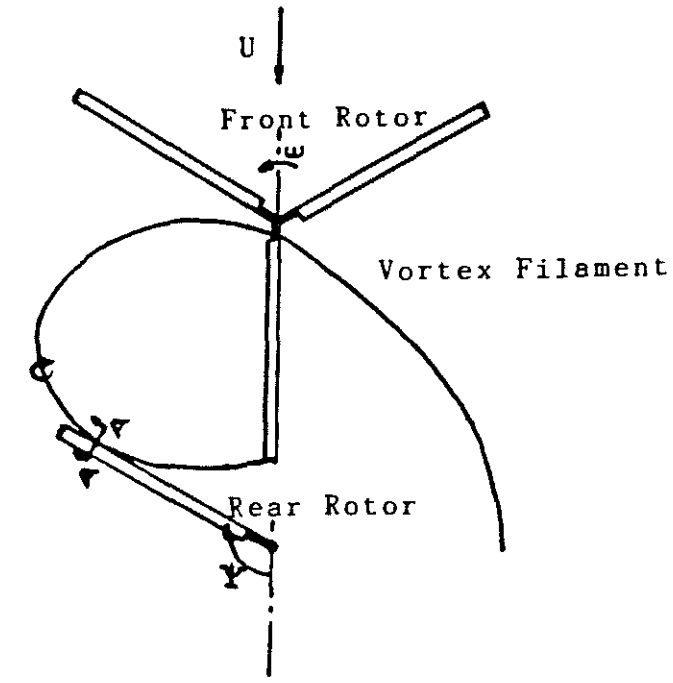

(a) Tandem Rotor

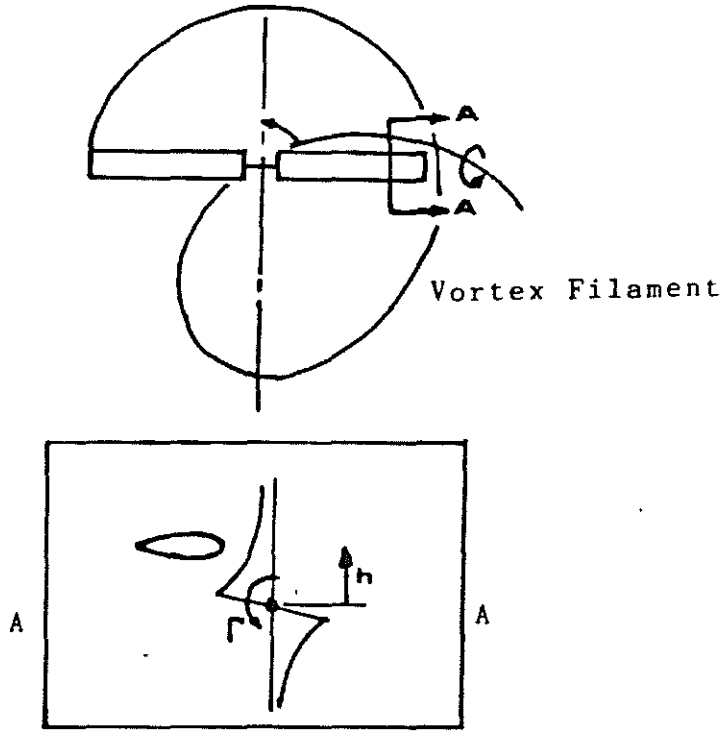

(b) Single Rotor

FIG. 1. PARALLEL BLADE VORTEX ENCOUNTER

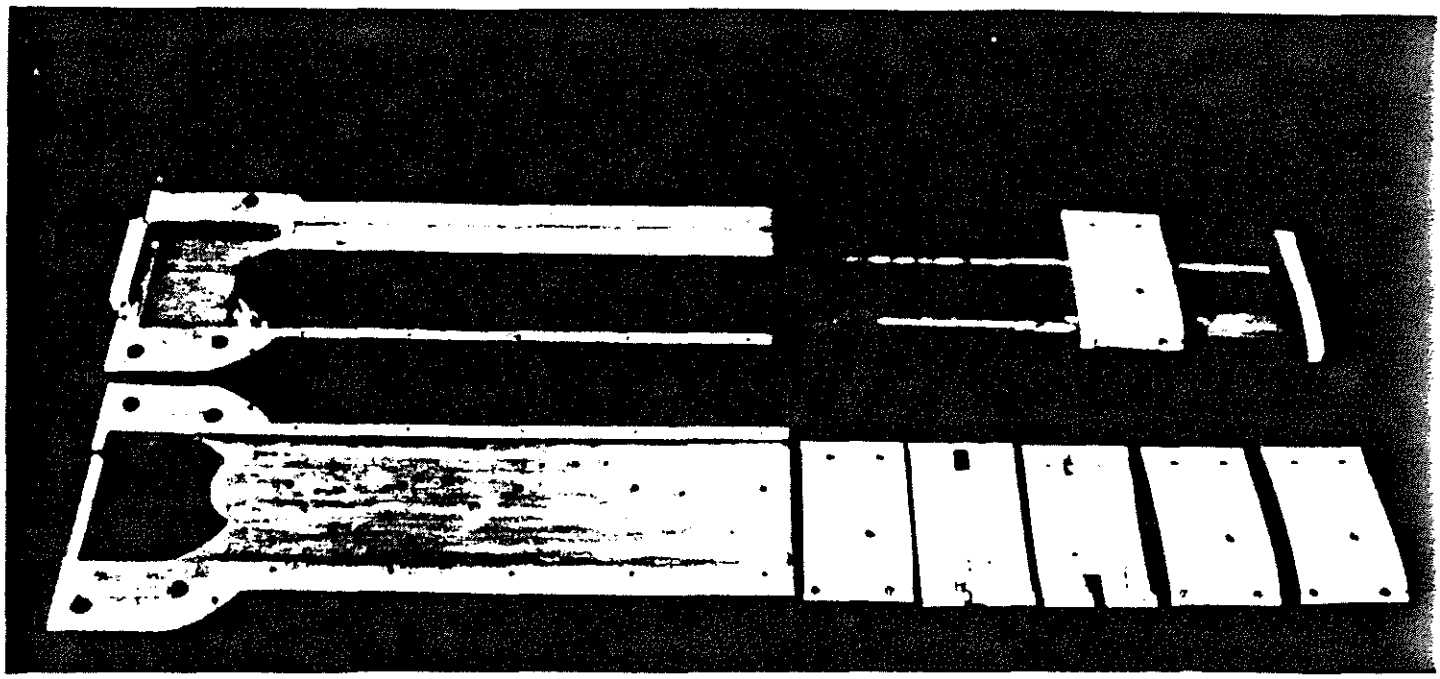

FIG. 4. ROTOR BLADE

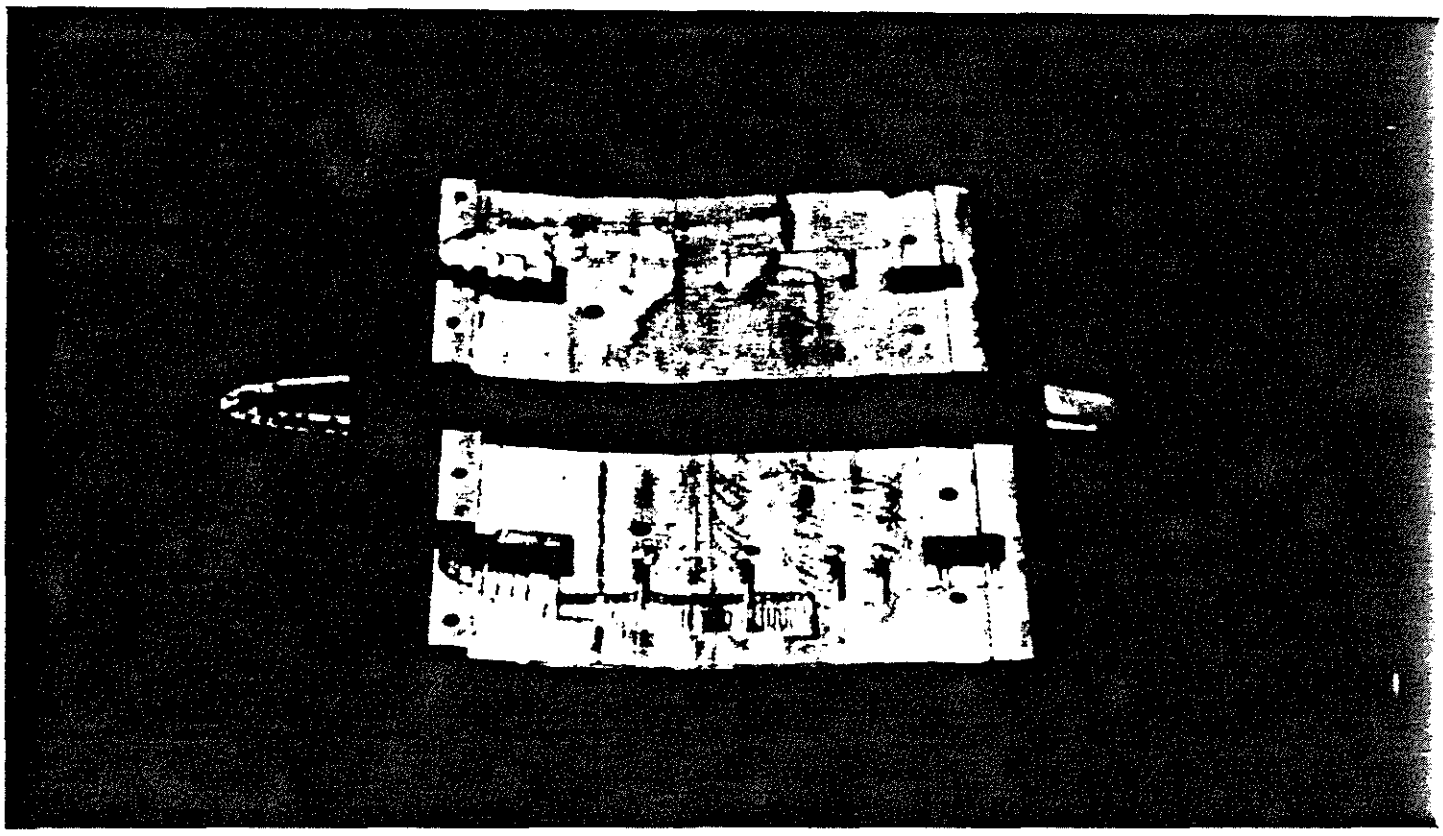

FIG. 5. INSTRUMENTATION POD

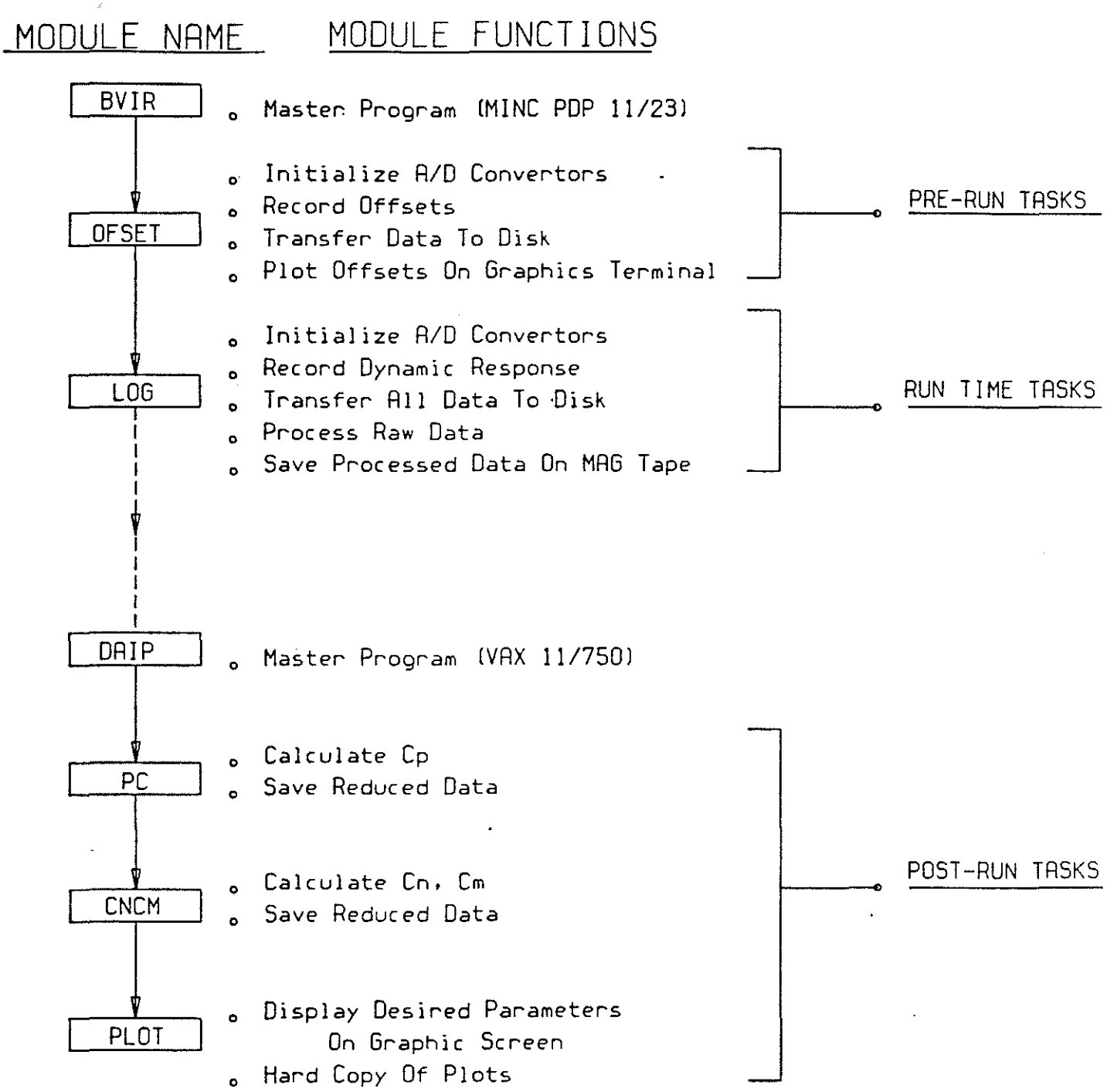

FIG. 7. MAJOR SOFTWARE TASKS

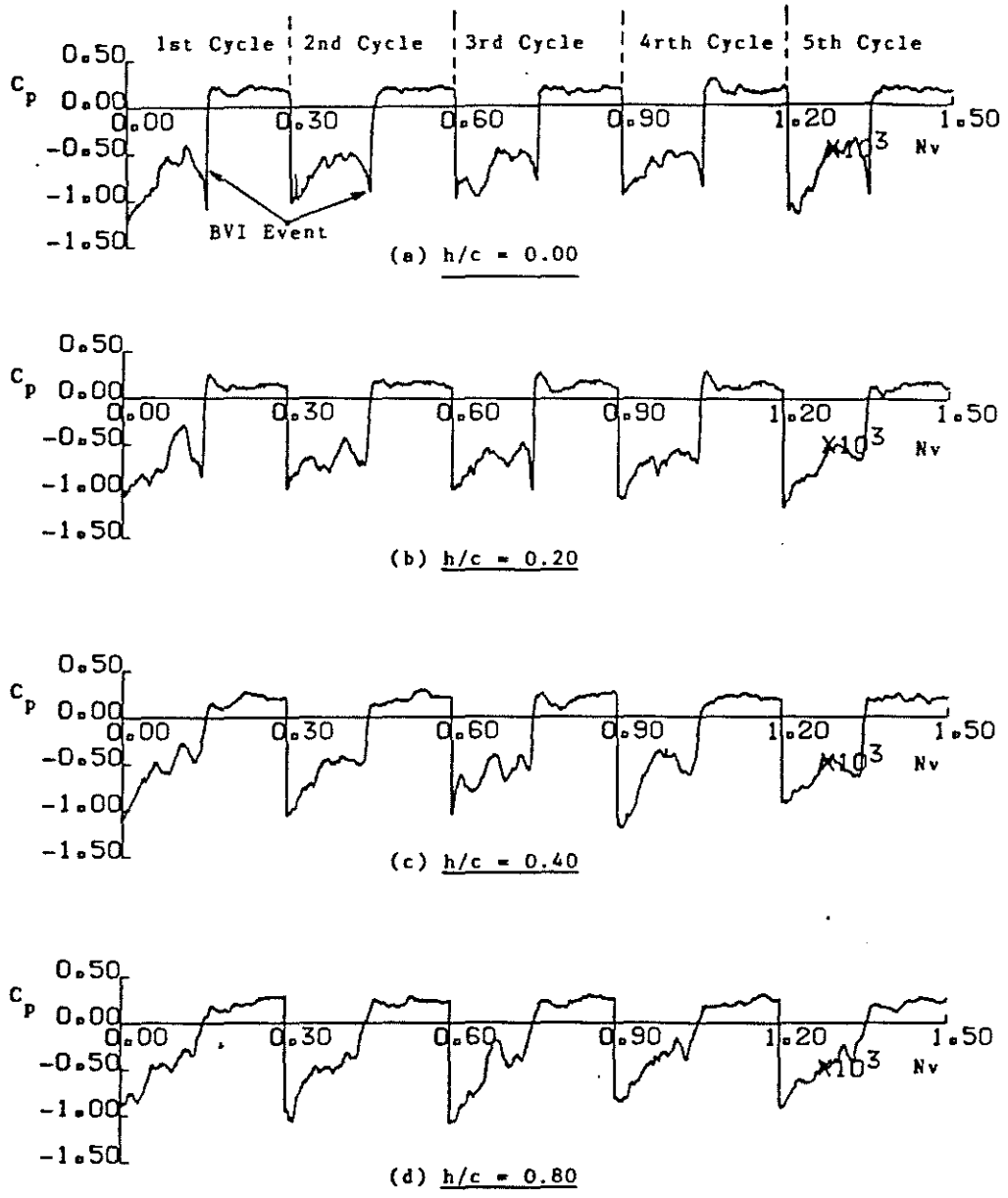

FIG. 9. TYPICAL PRESSURE COEFFICIENT TIME HISTORIES ($r/R=0.95$, $\delta=7.5°$)

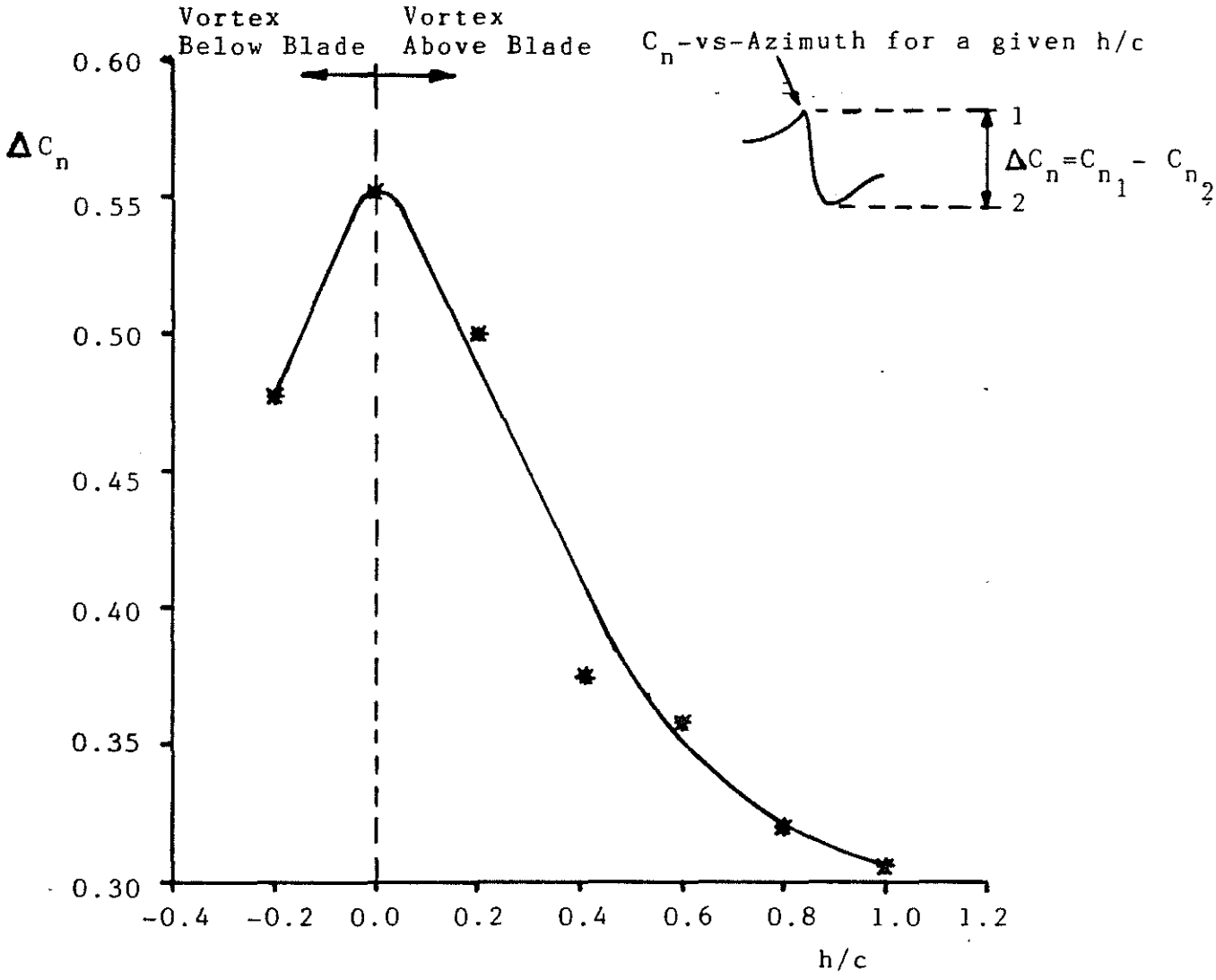

FIG. 11. THE EFFECT OF BLADE/VORTEX PROXIMITY ON MAXIMUM SECTION NORMAL FORCE COEFFICIENT (r/R=0.95, δ=7.5°)